INTERNATIONAL JOURNAL OF
COASTAL & OFFSHORE ENGINEERING
IJCOE Vol.1/No. 3/Autumn 2017 (1-8)

Available online at: http://ijcoe.org/browse.php?a_code=A-10-96-1&sid=1&slc_lang=en

The Effects of Internal Waves on Speed of Sound near Strait of Hormuz

Mojtaba Zoljoodi[1*], Afshin Mohseni Arasteh[2], Mojgan Ghazi Mirsaeid[3]

[1] Corresponding author: Faculty member and assistant professor, Iranian National Institute for Oceanography and Atmospheric sciences (INIOAS), email: zoljoodi@inio.ac.ir*
[2]Associated professor of Azad University, faculty of marine science and technology, North branch
[3]National Institute of Oceanography and Atmospheric Science

ARTICLE INFO

Article History:
Received: 30 Aug. 2017
Accepted: 20 Dec. 2017

Keywords:
Internal Wave
Sound Propagation
Vertical and Horizontal Movements

ABSTRACT

The internal waves complicate the propagation process of sound in the water. These waves are considered the main cause of disturbances in sound speed, and now it is known that the internal waves are the dominant parameter in the change process of sea frequency spectrum, as these changes range from many hourly cycles (floating frequency) to almost one daily cycle (inertia frequency).

The profile of mass sound speed in shallow waters depends on salinity and temperature gradients in turbulence internal waves. Here, the assumption is that the only probability function source is the turbulence internal waves in a water column. This investigation aims to use the mathematical models to study the internal wave effects on propagation of sound waves in shallow waters and that the waves how affect the sound propagation and depend on what parameters? We used the data gathered from Persian Gulf to calculate the parameters such as: sound speed, floating frequency, the ratio of resulted turbulences in sound propagation by vertical movement, phase functions and internal wave domain. Meantime, based on a given wave length (in the study area: 235 m.), the shape of first mode has been compared to the other modes. The probability density functions have been calculated for two different modes.

Comparing the ratio of generated turbulences in sound propagation by vertical movement and horizontal speed of particle, showed the horizontal movement is considerably less than the vertical one and also by increasing the depth (consequently decreasing the floating frequency), vertical movement is raised highly. The highest floating frequency and turbulences generated in sound propagation by vertical movement are found on the places near the water level and this is due to thermocline existence and on the other hand in the same places we have the lowest range of vertical movement.

1. Introduction

Marine environments mainly have the density stratification as they are in the forms of stepwise and continuous. While, the penetrative flow in the fluid with density stratification entered, the internal waves are generated and the penetrative flow energy propagates in vertical direction. Basically, the internal waves are existing in entire oceans but there is high probability of their existence in the gulfs and seas [1]. Sound waves regarding the energy transmission inside of the water is relatively stronger than the electromagnetism kinds [2]. So respect to the importance of both these waves in seas, this research investigates their effects in shallow waters.

2. The impact of internal wave turbulence on sound speed in shallow waters:

In shallow waters, the mean density is increasing by water depth linearly, so we have this function:

$$\bar{\rho}(z) = \rho_s + bz \quad (1)$$

where ρ_s is the water level density and b is the density gradient. Using the above relation and hydrostatic pressure formula, the pressure function in turbulence state is written as follows:

$$\bar{p}(z) = p_s + g(\rho_s + 1/2bz^2) \quad (2)$$

Where ρ_s is the atmosphere pressure, and g is magnetic velocity. But for shallow water, the above relation could be written as:

$$\bar{p}(z) = p_s + g\,\rho_s z \tag{3}$$

A function is presented by Ecart for the temperature as below:

$$\bar{T} = (2A)^{-1}[-B-(B^2-4AC)] \tag{4}$$

$$\begin{aligned} A &= -0.375 + 0.33625\bar{\rho} \\ B &= 38 - 37.424\bar{\rho} \\ C &= \bar{p}(1-0.698\bar{\rho}) + 5995 - 5831.01\bar{\rho} \end{aligned} \tag{5}$$

$\bar{T}$ in degree Celsius, $\bar{p}$ in atmosphere and $\bar{\rho}$ in gr/cm^3 are measured.

The speed of non-turbulent sound is calculated by below relation:

$$\begin{aligned} \bar{C}(z) = 0.3048[&4739.9 + 15\bar{T} - 0.1456\bar{T}^2 \\ &+0.01826 + 4.3(S-34)] \end{aligned} \tag{6}$$

And as we assumed the study area should be enough shallow the depth impact (z) could be ignored, as the below relation:

$$\bar{C}(z) = 0.3048[4739.9 + 15\bar{T} - 0.1456\bar{T}^2] \tag{7}$$

The mean sound speed profile could be calculated and plotted through the following provisions:

$\rho_s = 1.0223 gr/cm^3$, $p_s = 1at$, $H \approx 70m$.

The equation of vertical speed of internal wave with its boundary conditions, has been written as below:

$$\nabla^2 W_{zz} + N^2 \nabla_H^2 W + f^2 W_{zz} = 0 \tag{8}$$

$$W(x,y,0,t) = W(x,y,-D,t) = 0 \tag{9}$$

The above equation for a constant N^2, results as follows:

$$W = \varphi(z)\exp[i(kx + ly - \omega t)] \tag{10}$$

Where, $\varphi(z)$ is the range of vertical speed and ω is the internal wave frequency. $\varphi(z)$ Should be written as below in order to be applied in the relation of vertical speed of internal wave:

$$\varphi_n(z) = A_n \sin(n\pi z / D) \tag{11}$$

The index ***n*** shows the number of normal mode. The first mode has the high importance, as it includes usually the biggest range and shows low tension comparing to the high level modes. The internal wave frequency by wave length as: $L = 2\pi\left(k^2 + l^2\right)^{-1/2}$ could be changed to the below relation:

$$\omega_n = \left\{\left[4N^2 + (\frac{L}{H})^2 f^2 n^2\right]\left[4 + (\frac{L}{H})^2 n^2\right]^{-1}\right\}^{1/2} \tag{12}$$

The vertical speed while it is ***n=1*** by combining the relations (11) and (12), and separating its real section could be written as below:

$$W_1(x,y,z,t) = A_1 \sin(\frac{\pi z}{H})\cos(kx + ly - \omega_1 t) \tag{13}$$

The integration of relation (13) relative to the time results in the vertical movement as follows:

$$\gamma(x,y,z,t) = \Gamma \sin(z\pi / H)\sin(kx + ly - \omega_1 t) \tag{14}$$

Where, $\Gamma = -A_1/\omega_1$ has been considered the movement range. Thus for each following variables: *t*, *y*, *x*, the γ constant varies in the water column as sinusoidal.

The equations (4), (5) and (7), result in changes of temperature and sound speed profile. The variation of sound final speed is almost equal with the vertical movement of water multiplied by $\left(d\bar{C}/dz\right)$, so we have:

$$C_1(x,y,z,t) = \Gamma \frac{d\bar{C}}{dz}\sin(\frac{\pi z}{H})\sin(kx + ly - \omega_1 t) \tag{15}$$

And, the total speed of sound is written as:

$$\begin{aligned} C(x,y,z,t) &= \bar{C}(z) + \\ &\Gamma \frac{d\bar{C}}{dz}\sin(\frac{\pi z}{H})\sin(kx + ly - \omega_1 t) \end{aligned} \tag{16}$$

The above relation indicates the standard deviation of internal wave speed.

3. The interaction of sound wave accelerator and internal Solitons:

Orr and Baxter [3] based on ray theory worked on this issue and they studied the effect of ocean internal wave on short-range sound propagation and full frequency. The results revealed that the reaction of sound propagation frequency in shallow waters and summer time mostly depends on time and propagation direction and occasionally it illustrates a high weakness in some frequency domains. These waves exist in shallow waters as non-probability groups with given wave lengths and defined as alone waves or Solitons [4]. The transition of energy happens usually between the modes with special difference of its values could be equal to wave peak of internal wave spectrum or roughness of bed floor, it means:

$$k_{\text{int}} = \frac{2\pi}{\lambda_i} = k_n - k_m \tag{17}$$

Where, k_{int} is almost equal to special difference of values among normal acoustic modes. As an example:

$$\lambda_i = 235 \rightarrow k_{\text{int}} = \frac{2\pi}{235} = 0.026736 \qquad (18)$$

The equation below clearly indicates that why considerable amount of energy is transferred by the first mode to the high level modes and so why and where the frequency intensifying of acoustic wave and wave length of Solitons happen [Figure 1].

$$k_L L_p = \left(n + \frac{1}{2}\right)\pi \qquad (19)$$

L_p is the internal wave length [5].

Regarding to each special wave length (in the study area λ=235m.), the shape of first mode is quite different than the other modes, but about else wave lengths, the shapes are too close to the first mode. As a lot of energy is transferred from the first mode to the high level modes, in the longer waves the coupling effect of mode is considerably weak [6].

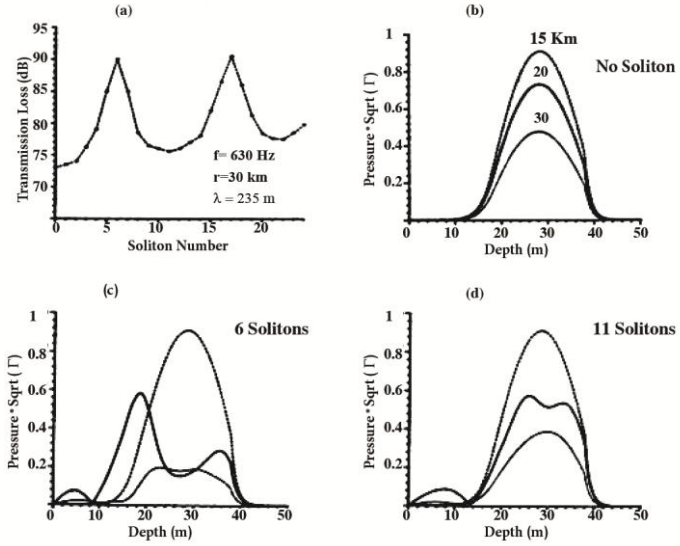

Figure 1. Intensifying of soliton wave length (a). Depth distribution function for various wave lengths (b-c-d) Zhou, Ji-Xun., 1991[۱].

4. Interaction of internal wave and acoustic in long-range

We assume internal wave movement could be written as below:

$$\eta(r,z,t) = \eta_D(r,z,t) + \eta_S(r,z,t) \qquad (20)$$

Where, η_D indicates the diffusion component and η_S is the Soliton portion [7].

At the moment, internal waves diffusion component in shallow waters is considered an important research topic. Diffusion field component is considered as a statistical combination from horizontal waves that is covered by Garret-Munk spectrum.

This issue uses a special orthogonal set of internal wave functions to expand $\eta_D(r,z,t)$, as it is obtained from linear equation of Navier-Stokes for stratified inviscid and sparse fluid. In this condition the diffusion field is defined as a weighted two fold summation on ***J*** number and horizontal wave number $(k_h = (k_x^2 + k_y^2)^{\frac{1}{2}})$:

$$\eta_D(r,z,t) = \sum_{k_h}\sum_{j} F(k_h, j) W(k_h, j, z) e^{i[k_h r - \omega(k_h, j)t}$$

(21)

In the relation above the average of weight factors are equal to zero.

Using k_h we assume that the internal wave field is homogenous horizontally. While, shear flow is considered negligible in the water column the diffusion relation $w(k_h, j)$ and special functions related to depth $W(k_h, j, z)$ in special equation of amount is applied as below:

$$\frac{d^2}{dz^2} W(z) + k_h^2 \left[\frac{N^2(z) - \omega^2}{\omega^2 - f_c^2}\right] W(z) = 0 \qquad (22)$$

Where, ***N*** is the floating frequency or Brunt-Vaisala frequency [8].

$$N^2(r,z) = -\frac{g}{\rho}\frac{\partial}{\partial z}\rho_p(r,z) = g\left(h\frac{\partial T_P}{\partial z} - s\frac{\partial s}{\partial z}\right) \qquad (23)$$

For the condition of rigid boundary we have as:
W(0)=W(H)=0.

Where, ***H*** is the water depth and the Coriolis frequency is obtained from the following relation: $f = 2\Omega\sin$ ◆ . Ω is the angle speed of earth. The results of equation (22) are independent from any range and so we ignore the coupling of internal wave mode that depends on the relation`s range with floating frequency. Now, by the result of partial equation range for coupling of acoustic mode, we are allowed to insert the dependence of range into the equation (21), whiles this dependency is applied for the bed by boundary condition. To simplification in the calculation of η_D the parameter of time has been taken into account equal to zero. This option revealed that the average values of acoustic field have been calculated by the samples which provide time intervals longer than the time to complete internal waves field (about many minutes).

As an instance; the floating frequency and sound speed profile have been calculated using the data sets of a device installed in the Persian Gulf at 2001 (Figure 2).

This profile illustrates the structure of a layer quasi waterway in a depth of 20m. by salinity and temperature gradient in a water column [9].

Special amount $w(k_h, j)$ and special functions $W(k_h, j, z)$ are calculated by equation (22) in a domain $k_h\{0.0002, 0.25\}m^{-1}$ which is correspondent to horizontal wave length from 25 to 31/4 km. Such range of wave covers spatial scales which are important for acoustic calculations in this investigation. The depth of water has been taken into account about H=70m. and the latitude of 30° N is chosen for coriolis frequency measurement.

The exponential spectrum that is related to $F(k_h, j)$ has been assumed as Garrett-Munk spectrum [10]:

$$<|F(k_h, j)|^2> = E_0 M [j^2 + j_*^2]^{\frac{-p}{2}} (\frac{4}{\pi}) k_j k_h^2 (k_h^2 + k_j^2)^{-2} \quad (24)$$

The quantity of k_j is obtained by $k_j = (\pi i f_c) / \int_0^H N(z)dz$ and for j[th] mode with the spectrum peak is related to dominant horizontal wave number. The normalize parameter of ***M*** defined by $\frac{1}{M} = \sum_{j=1}^{x} [j^2 + j_*^2]^{\frac{-p}{2}}$. The parameter of E_0 indicates the average of energy density (J/m^2) and it is in relation with the exponent of internal wave oscillation. The features of wave number as j_*, and exponent of spectrum as ***P*** experimentally define the parameters which control the relative modes of internal waves.

The amount of E_0 in most of simulations is $۲۵ J/m^2$, it means that 10% of E_0^{max} has been chosen and it is physically rational. The weight factor of mode (p) is considered [8].

An example of sound speed fluctuations δc that is in relation to the field of diffusion internal wave η_D has been shown in figure 3 with the sound speed component. These fluctuations depend on both depth and range. The variations of depth and range averages are calculated by mean sound speed $<(\delta c / c)^2> \approx 0.5(10^{-6})$. The fluctuations are restricted to an area of thermocline where maximum share of temperature and salinity are floating on frequency whiles the high level modes have relatively smaller shares on the total spectrum and in understanding of acoustic diffusion are considered so important, as vertical structure of high level modes generate much more acoustic diffusion comparing to the low level modes as well as the modes without structure.

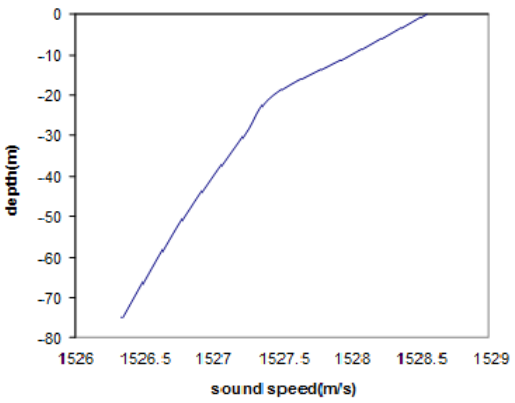

Figure 2. Calculation of sound speed profile using the data sets of a device installed near Hormuz Strait at 2001.

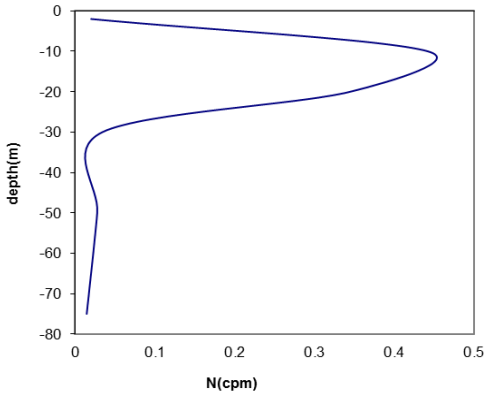

Figure 3. Calculation of buoyancy frequency using the data sets of a device installed in the Persian Gulf near Hormuz Strait at 2001.

In total, both domains of condition and phase influence the pressure field. On the other hand the calculations of deviation and mode velocities in the share of phase are negligible. Thus we have the relation as follows:

$$I_i(n, r, f) = d_i^* c(n, r, f) d_i(n, r, f) \quad (25)$$

The comparison of the obtained deviation coefficients indicates that the domain calculation only by considering 10 first modes includes many quality characteristics in entire field for the shortest ranges [Figure 4].

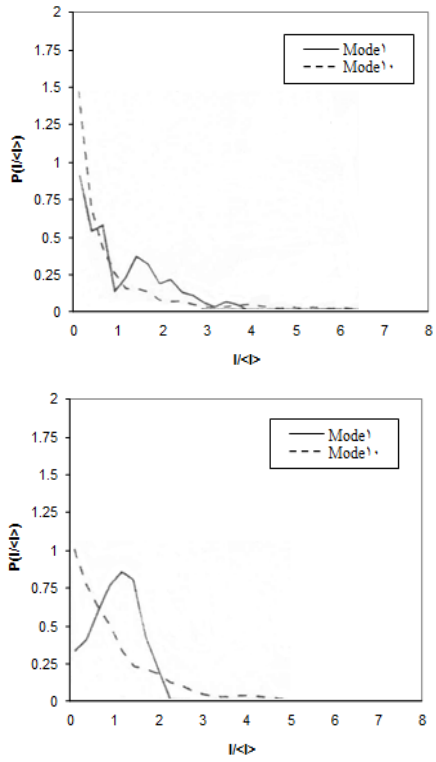

Figure 4. Probability density functions $Q(I_i(n,r,f)/<I_i(n,r,f)>)$ for the modes 1 and 10 (left) r=20km and (right) r=200km. in both cases density energy E0=100J/m^2 and the installation depth of assumed source is at 45m.

5. The mathematical model of internal wave effect on sound diffusion

The mathematical model is presented as below to consider the internal wave impacts on sound diffusion [11]. In this method the equation of acoustic wave pressure fluctuation is applied.

$$\nabla^2 P + \left(\omega_0^2/c^2\right)P = 0 \tag{26}$$

By writing $k = \omega_0/c_0$ and $\left(\omega_0/c\right)^2 = \omega_0^2/\left(c_0+\delta c\right)^2 \cong \left(\omega_0/c_0\right)^2\left(1+2\mu\right)$ and replacement of $P = p\exp\left(i\ 2\pi kx\right)$ in the equation (22) we will have:

$$\nabla^2 p + 2i2\pi k\partial_x p + 2\mu\left(2\pi k\right)^2 p = 0 \tag{27}$$

To define domain and phase of wave the relation below has been used:

$$p = e^{\psi} = Ae^{is} \quad ,i.e.\ .\ , \qquad \psi = \ln A + iS \equiv \chi + iS \tag{28}$$

The above relation will change the equation (27) as below:

$$\nabla^2\psi + 2\ i\left(2\pi k\right)\partial_x\psi + 2\left(2\pi k\right)^2\mu = -\left(\nabla\psi\cdot\nabla\psi\right)^2 \tag{29}$$

Ignoring the non-linear phrases and through Fourier transform:

$$\mu\left(x,z,r\right) = \int d\beta\, d\omega\, v\left(x;\beta,\omega\right)\exp\left[2\ i\pi\left(\beta z - \omega t\right)\right] \tag{30}$$

$$\psi\left(x,z,t\right) = \int d\beta\ d\omega\ \bar{\psi}\left(x;\beta,\omega\right)\exp\left[2\ i\pi\left(\beta z - \omega t\right)\right] \tag{31}$$

So based on above relations, it is changed to a normal differential equation in terms of $\bar{\psi}$

$$\left[\partial_{xx}^2 + 2\ i\left(2\pi k\right)\partial_x - \left(2\pi\beta\right)^2\right]\bar{\psi} = -2(2\pi k)v \qquad \bar{\psi}\left(x=0;\beta,\omega\right) = 0 \tag{32}$$

The Fourier transform of phase (s) and domain (χ) is written as below:

$$\bar{s}\left(x;\beta,\omega\right) = \left(1/2i\right)\left[\bar{\psi}\left(\beta,\omega\right) - \bar{\psi}^*\left(-\beta,-\omega\right)\right], \tag{33-a}$$

$$\bar{\chi}\left(x;\beta,\omega\right) = \frac{1}{2}\left[\bar{\psi}\left(\beta,\omega\right) + \bar{\psi}^*\left(-\beta,-\omega\right)\right], \tag{33-b}$$

And as $\bar{v}^*\left(-\beta,-\omega\right) = \bar{v}\left(\beta,\omega\right)$, so we have:

$$\begin{Bmatrix}\bar{s}\\ \bar{\chi}\end{Bmatrix} = 2k\pi\int_0^x \bar{v}\left(x';\beta,\omega\right)\begin{matrix}\cos\\ \sin\end{matrix}\left[\frac{\pi\beta^2\left(x-x'\right)}{k}\right]dx' \tag{34}$$

$$<\mu^2> = \int_f^n d\omega\int_0^\infty d\beta\ \varphi_\mu\left(\omega,\beta\right) \tag{35}$$

And φ_μ is obtained by Garret-Munk model.

Thus, the index of diffraction spectrum will be resulted as follows [Figure 10]:

$$\Phi_\mu\left(\omega,\beta\right) = 2\times\left(\frac{2}{\pi}\right)^2\left\langle\mu^2\right\rangle f\,\frac{\left(\omega^2-f^2\right)}{\beta_*\omega^3}\,\frac{1}{\left[1+\left(\frac{\beta}{\beta_*}\right)^2\right]}$$

$$\begin{cases}\left\langle\mu^2\right\rangle = G\ n^2\left\langle\xi^2\right\rangle\\ \beta_* = t\left(n^2-\omega^2\right)^{\frac{1}{2}}\end{cases} \tag{36}$$

Also, similarly about φ_s we will have as [Figures 6 and 9]:

$$\begin{matrix}\varphi_S\left(\omega;\beta\right)\\ \varphi_\chi\left(\omega;\beta\right)\end{matrix} = 4\left(K/\beta\right)^4\varphi_\mu\left(\omega,\beta\right)\Im_\pm\left(\tilde{L},\Gamma\right) \equiv \mathrm{N}_\pm\varphi_\mu \tag{37}$$

Where:

$$\pm \equiv \int_0^{\tilde{L}} d\eta \; J_0(\Gamma\eta) \left[\left(\tilde{L}-\eta\right)\cos\eta \pm \cos\tilde{L}\sin\left(\tilde{L}-\eta\right)\right] \quad (38)$$

[Figures 7 and 8]

$$\tilde{L} = \pi\beta^2 L / k$$

$$\Gamma = \left(\frac{2k}{\beta}\right)\left[\left(\omega^2 - f^{\,2}\right)/\left(n^2-\omega^2\right)\right]^{\frac{1}{2}}$$

$$N_{\pm} \equiv 4\left(k/\beta\right)^4 \Im_{\pm} \quad (39)$$

$$\Im_{\pm} = \begin{cases} \left(\tilde{L} \pm \cos\tilde{L}\sin\tilde{L}\right)/\Gamma \\ 2\tilde{L}/\Gamma & \tilde{L} << 1 \\ 2\tilde{L}^3/(3\Gamma) & \\ \tilde{L}/\Gamma \quad \tilde{L} >> 1 \end{cases}$$

To calculate the max and min values of β, the Richardson Number is used . For simplifying of calculations, the frequencies relating to internal waves in *cph* and the acoustic signal frequencies in *Hz* are used.

Using their models, the produced disturbances by internal waves, domain spectrum and relative phase to vertical wave number, internal wave spectrum to vertical wave number and domain function and phase are calculated for a selected station in the Persian Gulf with geographic position of 27° 28`.50 N and 51°57`.01E , in 2001 marine cruise.

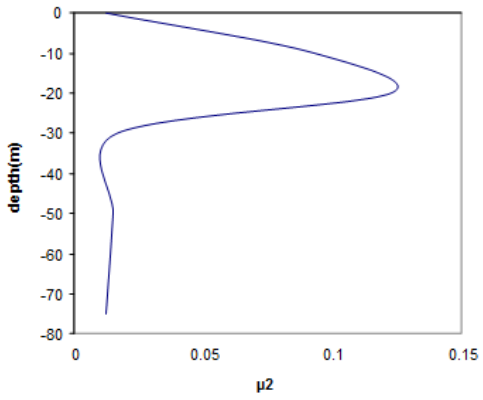

Figure 5. The produced disturbances by internal wave in vertical speed

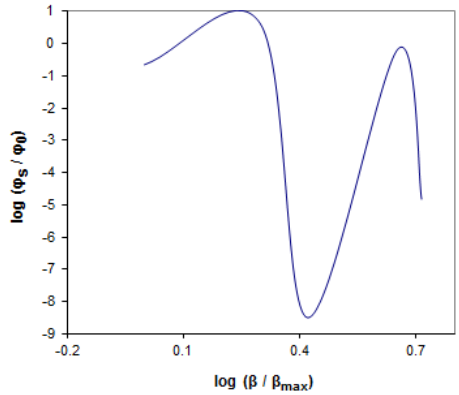

Figure 6. Phase spectrum into the vertical wave number

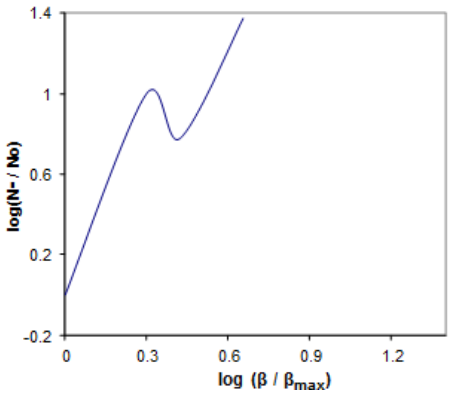

Figure 7. The function domain into vertical wave number

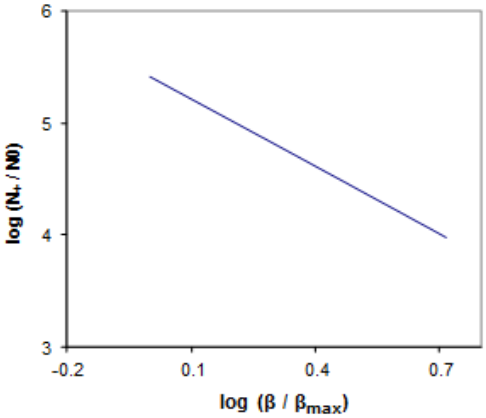

Figure 8. The phase function into vertical wave number

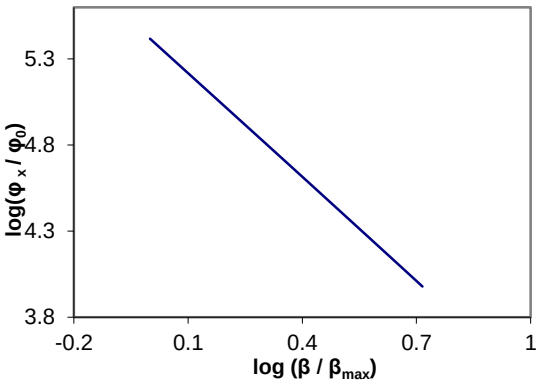

Figure 9. The domain spectrum into vertical wave number

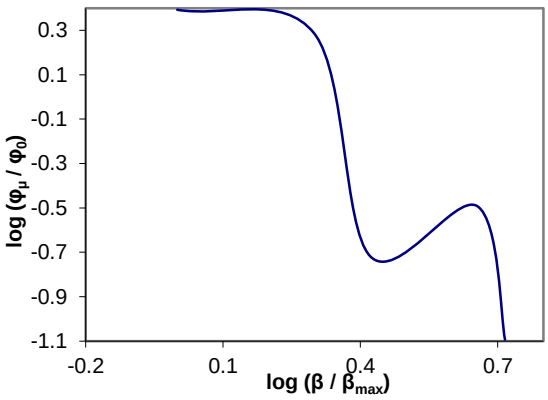

Figure 10. Internal wave spectrum into vertical wave number

Table 1. The sample of calculations for data derived from a sample station in the Persian Gulf near Strait of Hormuz , in 2001 marine cruise.

Depth(m)	μ^2	sound speed(m/s)	N(cpm)	log(N-/N0)	$\log(\beta/\beta_{max})$	$\log(\varphi_x/\varphi_0)$	$\log(\varphi_s/\varphi_0)$	$\log(\varphi\mu/\varphi 0)$	$\log(N_+/N_0)$
-10	9.29E-02	1528.005	0.4418472	-0.107634	0	5.4161	-0.657052	0.393397	5.4161
-20	1.23E-01	1527.438	0.3448281	0	0.2995	4.8164	0.612442	0.285728	4.8164
-30	1.64E-02	1527.225	0.0342646	1.0013114	0.4212	4.5721	-8.497586	-0.717028	4.5721
-50	1.49E-02	1526.792	0.0576210	0.7762278	0.6549	4.1009	-0.165614	-0.491293	4.1009
-75	1.22E-02	1526.340	0.0144245	1.3748308	0.7158	3.9773	-4.824745	-1.0927730	3.9773

6. Conclusion and discussions

- Regarding to the increase of energy density amount of the internal wave, the further fluctuation of sound speed and the regular stronger coupling mode are generated. In general, the attenuation amount of each especial mode depends on the coupled modes and also weakening coefficient of mode.
- Studying the different wave-lengths, shows that in a given wave-length the first mode shape is quite distinct than the other modes, whiles about the other wave lengths, the mode shapes are too similar to the first mode. Accordingly, the big amount of energy is transferred from the first mode to the high level modes, but in the higher boxes, the coupling effect of mode is very weak.
- Since, the acoustic phase of linear function is generated from internal wave movement, the domain fluctuation is resulted from intervention of many rays.
- If the share of internal wave field spectrum is by random, the domain and range also will be random. Understanding this question is important that the phase spectrum is proportionate with the internal wave spectrum, but the domain spectrum includes the frequentative components by the generated frequency change from internal wave. Thus when the domain and phase spectrums are random, so the phase information is belonging to the environmental parameters, whiles it is not so about the domain.
- The phase spectrum decreases with the internal wave frequency cubic and it is compatible with acoustic frequency range and root. The domain spectrum also similarly decreases with the internal wave frequency cubic. But it is independent from the acoustic frequency and range cubic. All these results are compatible with the theories. But relating to the phase it is also consistent with the available data.
- The biggest amount of floating frequency and the produced disturbances in the sound propagation because of vertical movement are shown on the area near to the water level and on the other hand in the same place the lowest vertical movement is happened, as the vertical movement increases as $n^{-1/2}$ with depth. Therefore, by the equation of $\mu = n^2(z)\zeta\sigma / g$, the fluctuation of sound speed by depth increases with the exponent 3/2 of floating frequency $\left(n^{3/2}\right)$.
- The biggest amount of floating frequency (N) is in the thermocline area and the lowest beside the bed, is available.
- Comparing the above graphics indicated that the internal wave floating frequency can affect the sound wave frequency. In first 20 meters of depth where the sound speed decrease rapidly, the floating frequency is maximum because of some formation principals of the water masses and density gradient, and consequently the highest disturbances in sound speed happed. The density gradient by depth increasing is weakening and consequently the floating frequency and generated disturbances in sound speed is minimized through the internal waves.
-
- **References**

1- Zhou, Ji-Xun., (1991), *Resonant interaction of sound wave with internal solitons in the coastal zone*, J. Acoust. Soc. Am.90(4), 2042-2053.

2- Tielburger, D., Acou.Y. f., (1997), *Propagation through an internal wave field in a shallow water waveguide* , J. Acoust. Soc. Am.101(2), 789-807.

3- Orr, M. H., Baxter, L. and Hess, F. R., (1980), *Remote acoustic sensing of the particulate phase of industrial chemical wastes and sewage sludg*, Woods Hole Oceanogr.Inst., Woods Hole, mass., WHO1 Tech. Rep. 79-38, 153pp.

4- Desaubies, Y. f.,(1976), *Acoustic-phase fluctuation induced by internal waves in the ocean*, J. Acoust. Soc. Am.60(4), 795-800 .

5- S. M., 1975, " Effects of internal waves on sound pulse propagation in the straits of florida," J. Acoust. Soc. Am.58(6),1151-1158.

6- Bates, B. J., (1987), *Stochastic simulation and first-order multiple scatter solutions for acoustic propagation through oceanic internal waves*, J. Acoust. Soc. Am. 82 (6), 2042-2049.

7- Small, J. and Martin, J., (2002), *The generation of non-linear internal waves in the Gulf of Oman. Continental shelf research*, 22(8): 1153-1182.

8- Thorpe, S. A., (2005), *The turbulent ocean*, Cambridge University Press.pp 230.

9- Jackson, C., (2007), *Internal wave detection using the Moderate Resolution Imaging Spectroradiometer* (MODIS), J. Geophysical Research, VOL. 112, C11012.

10- Mohseni, A., Chegini v., Mirsaeid M., (2010), *A mathematical model of internal waves on sound (case*

study Caspian Sea), J. of Iranian marine science and technology, No.4, P.92-103.
11- Muacho, S., da Silva, J. C. B., Brotas, V. and Oliveira, P. B., (2013), *Effect of internal waves on near-surface chlorophyll concentration and primary production in the Nazaré Canyon (west of the Iberian Peninsula).* Deep Sea Research Part I: Oceanographic Research Papers 81(0): 89-96.